Meiotic HORMA domain proteins prevent untimely centriole disengagement during *Caenorhabditis elegans* spermatocyte meiosis

Mara Schvarzstein[a,1], Divya Pattabiraman[a], Joshua N. Bembenek[b], and Anne M. Villeneuve[a,1]

[a]Departments of Developmental Biology and Genetics, Stanford University School of Medicine, Stanford, CA 94305; and [b]Department of Biochemistry, Cellular, and Molecular Biology, University of Tennessee, Knoxville, TN 37916

Edited by R. Scott Hawley, Stowers Institute for Medical Research, Kansas City, MO, and approved January 16, 2013 (received for review August 10, 2012)

In many species where oocytes lack centrosomes, sperm contribute both genetic material and centriole(s) to the zygote. Correct centriole organization during male meiosis is critical to guarantee a normal bipolar mitotic spindle in the zygote. During *Caenorhabditis elegans* male meiosis, centrioles normally undergo two rounds of duplication, resulting in haploid sperm each containing a single tightly engaged centriole pair. Here we identify an unanticipated role for *C. elegans* HORMA (Hop1/Rev7/Mad2) domain proteins HTP-1/2 and HIM-3 in regulating centriole disengagement during spermatocyte meiosis. In *him-3* and *htp-1 htp-2* mutants, centrioles separate inappropriately during meiosis II, resulting in spermatids with disengaged centrioles. Moreover, extra centrosomes are detected in a subset of zygotes. Together, these data implicate HIM-3 and HTP-1/2 in preventing centriole disengagement during meiosis II. We showed previously that HTP-1/2 prevents premature loss of sister chromatid cohesion during the meiotic divisions by inhibiting removal of meiotic cohesin complexes containing the REC-8 subunit. Worms lacking REC-8, or expressing a mutant separase protein with elevated local concentration at centrosomes and in sperm, likewise exhibit inappropriate centriole separation during spermatocyte meiosis. These observations are consistent with HIM-3 and HTP-1/2 preventing centriole disengagement by inhibiting separase-dependent cohesin removal. Our data suggest that the same specialized meiotic mechanisms that function to prevent premature release of sister chromatid cohesion during meiosis I in *C. elegans* also function to inhibit centriole separation at meiosis II, thereby ensuring that the zygote inherits the appropriate complement of chromosomes and centrioles.

Sexual reproduction relies on the production of complementary gametes that together contribute all of the components necessary for normal embryonic development. In many animal species, each gamete provides the zygote not only with a haploid complement of chromosomes but also with complementary components of the centrosome. Centrosomes are organelles that nucleate and help to organize microtubule arrays within the cell. Each centrosome contains either one or two cylindrical microtubule structures called centriole(s), which recruit pericentriolar material (PCM) to form a functional centrosome. A prevalent scheme to ensure that gametes provide complementary contributions of centrosome components to the zygote is to selectively dispose of either the centrioles or the pericentriolar material by the end of gametogenesis (reviewed in ref. 1). In most animals, developing oocytes typically eliminate their centrioles before the meiotic divisions. As a result, segregation of meiotic chromosomes in oocytes takes place on acentrosomal (anastral) spindles. Conversely, developing spermatocytes retain functional centrosomes throughout their meiotic divisions and then selectively discard the PCM once they have completed their meiotic divisions (1). Following fertilization, sperm-contributed centrioles recruit PCM from the oocyte to form the first centrosome of the embryo. Thus, maintaining the correct organization of centrioles during male meiosis is key to ensuring formation of a normal bipolar mitotic spindle in the zygote.

During the mitotic cell cycle, centriole duplication parallels DNA replication and cell division in that it occurs only once per cell cycle (recently reviewed in ref. 2). Centriole duplication begins at the G1 to S transition of the cell cycle, when a new (daughter) centriole begins to form orthogonally adjacent to each of the two centrioles inherited from the previous cell division. Each daughter centriole remains engaged with its parent centriole until late in mitosis or early in G1 phase (3), after chromosome segregation has taken place. Loss of the physical link maintaining the orthogonal relationship between parent and daughter centrioles, a step referred to as "disengagement," is important for licensing the initiation of the next duplication cycle of the centrioles (4, 5).

The fact that meiosis involves two rounds of cell division following a single round of DNA replication necessitates a modification of the centriole cycle: centrioles must either undergo one additional round of duplication in the absence of an S phase or undergo the meiosis II division with centrosomes containing a single unduplicated centriole. In *C. elegans,* as in mammals, centrioles undergo two rounds of duplication during male meiosis (Fig. 1*A*). The centriole pairs must disengage before each round of duplication, and disengaged parent centrioles each grow a new engaged daughter centriole (Fig. 1*A*). However, whereas centriole pairs disengage at anaphase of meiosis I, centriole pairs remain engaged at the end of the second meiotic division, so that each resulting haploid sperm has a tightly engaged centriole pair, typically visible as a single focus by immunostaining of centriolar proteins (Fig. 1*B*) (6–8). Upon fertilization, the centriole pair remains engaged and associated with the sperm chromatin mass while the female meiotic divisions resume. Once female meiosis has progressed to anaphase II, the paternally provided centriole pair separates and start to accumulate the maternally contributed PCM (7, 9). Each of these separated centrioles starts to form an orthogonal daughter centriole after female meiosis has been completed, as the female pronucleus migrates posteriorly toward the male pronucleus (7, 9–11). These newly formed centrosomes organize the first mitotic spindle of the embryo, and their centrioles serve as the parental centrioles in the subsequent division.

In this work, we identify an unanticipated role for *Caenorhabditis elegans* HORMA (Hop1/Rev7/Mad2) domain–containing proteins HTP-1/2 and HIM-3 in regulating centriole dynamics during spermatocyte meiosis. The conserved meiosis-specific HORMA domain proteins are components of specialized chro-

Author contributions: M.S. and A.M.V. designed research; M.S. and D.P. performed research; M.S. and J.N.B. contributed new reagents/analytic tools; M.S. and A.M.V. analyzed data; and M.S. and A.M.V. wrote the paper.

The authors declare no conflict of interest.

This article is a PNAS Direct Submission.

[1]To whom correspondence may be addressed. E-mail: maras1@stanford.edu or annev@stanford.edu.

See Author Summary on page 3727 (volume 110, number 10).

This article contains supporting information online at www.pnas.org/lookup/suppl/doi:10.1073/pnas.1213888110/-/DCSupplemental.

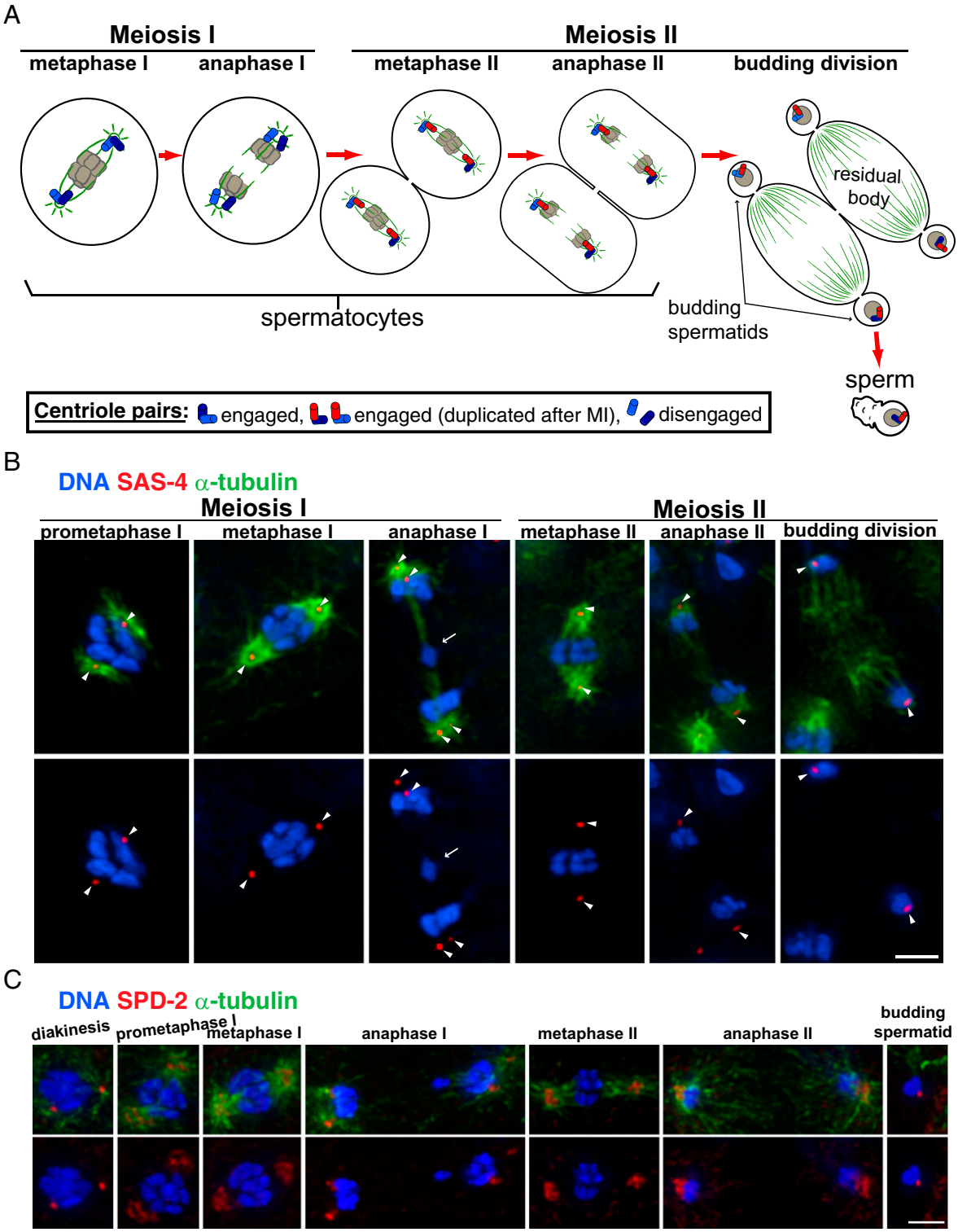

Fig. 1. Spermatocyte meiotic divisions. (*A*) Schematic diagram illustrating the centrosome duplication cycle and organization of centrioles during the spermatocyte meiotic divisions (this work and refs. 6 and 31). The first centriole duplication occurs early in prophase I (Fig. S1) so that metaphase I spindles have an engaged centriole pair at each pole (6). Centriole pairs disengage early in anaphase I, concurrently with chromosome segregation (*B*). A second round of centriole duplication is completed before metaphase II. Mother and daughter centrioles are represented in two different shades of blue in the first meiotic division. Daughter centrioles generated in the second centriole duplication are in red. Centriole pairs at each aster remain engaged during metaphase II, anaphase II, and cytokinesis II (budding division), when each engaged centriole pair guides the budding of a spermatid. During budding, microtubules and many other spermatocyte components are discarded into the residual body. The centriole pair remains engaged in mature sperm and does not become disengaged until after fertilization. (*B* and *C*) Projections of immunofluorescence images of spermatocytes stained with anti–α-tubulin, Hoechst, and α-SAS-4 (which localizes specifically to centrioles; *B*) or α-SPD-2 (which localizes both to centrioles and to pericentriolar material during some stages of the cell cycle; *C*). Arrowheads in *B* indicate single centriole foci corresponding to engaged centriole pairs, whereas pairs of arrowheads at anaphase I indicate separated centrioles; arrows indicate lagging chromosomes (likely the X) at anaphase I. (Scale bars, 2 μm.)

mosomal structures known as axial elements that assemble along the lengths of sister chromatid pairs during meiotic prophase I (12). In the context of meiotic prophase I, members of the HORMA protein family have been implicated in promoting homolog recognition, in loading of meiotic cohesion complexes, in regulating assembly of the synaptonemal complex, in promoting initiation of meiotic recombination and/or inhibiting recombination between sister chromatids, and in the operation of checkpoint-like mechanisms that coordinate several key prophase I events (13–19).

Most relevant for the current work, we previously identified a role for *C. elegans* HTP-1/2 in regulating two-step loss of sister chromatid cohesion during the meiotic divisions (20). In meiosis, homologous chromosomes segregate away from each other in the first division, whereas sister chromatids are segregated to opposite spindle poles in the second division (reviewed in ref. 12). The two (maternally and paternally derived) homologs are temporarily held together by chiasmata, physical linkages between the homologs that results from crossover recombination events between their DNA molecules in conjunction with sister chromatid cohesion flanking the crossover site. Segregation of homologs at meiosis I requires the release of a subset of cohesion to remove these connections while retaining localized cohesion between sister chromatids until the second meiotic division. Sister chromatids orient away from each other and segregate to opposite spindle poles at meiosis II. In organisms with localized centromeres (monocentric), two-step loss of sister cohesion is accomplished through pericentromeric protection of cohesion during meiosis I (21). Cohesion protection in meiosis I is mediated by the MEI-S332/Shugoshin-PP2A-B′ complex (22–24), which antagonizes cohesin loss by removing phosphate groups that target the meiosis-specific REC-8 component of cohesin for cleavage by the cysteine-protease separase (23, 25). Organisms such as nematodes that have holocentric chromosomes also protect cohesin from removal locally to accomplish loss of sister chromatid cohesion in two steps (reviewed in ref. 12). However, regulation of cohesin removal in *C. elegans* meiosis does not require Shugoshin. Instead, the HTP-1/2 and LAB-1 proteins become localized during late prophase to the domains where cohesin complexes containing the meiosis-specific subunit REC-8 will be retained at meiosis I, where they function in a Shugoshin-independent mechanism to inhibit premature loss of cohesion by inhibiting REC-8 removal (20, 26).

There are several logical parallels between (*i*) the requirement to prevent loss of sister chromatid cohesion at anaphase of meiosis I and (*ii*) the requirement to prevent centriole disengagement at anaphase of meiosis II. In both cases, preventing the untimely separation of two identical structures (i.e., sister chromatids or centriole pairs) during the meiotic divisions is necessary to avert aberrant subsequent divisions. Further, both of these features represent departures from the mitotic cell cycle program, in which both separation events occur at or soon after each anaphase. In this work, we discovered that these are not simply logical parallels, but reflect operation of the same meiosis-specific mechanism. In the course of imaging newly fertilized zygotes produced by *him-3* and *htp-1/2* mutants, we found that a subset of early embryos harbored extra centrosomes. Through the analysis presented here, we show evidence that this centriole disregulation reflects a role for meiosis-specific HORMA proteins HIM-3 and HTP-1/2 in inhibiting disengagement of centrioles at anaphase II of spermatocyte meiosis. Our data suggest a mechanistic parallel between meiosis-specific regulation of centriole and sister chromatid separation, both depending on HORMA-dependent protection of REC-8 cohesin from separase-dependent removal.

Results and Discussion

High-Resolution Imaging of Centrosomal Proteins During WT Spermatocyte Meiosis. To set the stage for our analysis of the mechanisms that inhibit centriole separation in *C. elegans* secondary spermatocytes and sperm, we present schematics and high-resolution images of the WT spermatocyte meiotic divisions in Fig. 1. In Fig. 1*B*, centrioles are visualized by immunofluorescence (IF) detection of SAS-4, a centriolar protein (27). During most stages of the spermatocyte meiotic division program, a single centriole focus is usually detected at each spindle pole; the exception is anaphase I, when two separated centriole foci are detected at each spindle pole. Prior EM analyses indicated that the first centriole duplication takes place before metaphase I and that the second centriole duplication occurs between metaphase I and metaphase II, because engaged centriole pairs were observed at each centrosome of metaphase spermatocytes in both meiotic divisions (as shown in Fig. 1*A*) (6). Our imaging shows that SAS-4 centriole foci separate at the metaphase I–anaphase I transition, indicating that chromosome separation in the first meiotic division is concurrent with the centriole separation event of the second centriole duplication cycle of spermatocyte meiosis (Fig. 1*B*).

We also used IF to evaluate the state of the coiled-coil domain containing protein SPD-2 (Fig. 1*C*; Fig. S1). In mitosis, SPD-2 localizes both to the immediate vicinity of the centrioles and to the PCM and is essential for centrosome maturation (i.e., recruitment of microtubule-nucleating γ-tubulin complexes to the PCM) and centrosome duplication (28–30). Our imaging of SPD-2 in male germ lines (Fig. S1) indicates that centriole disengagement, which is required to license duplication, occurs early in meiotic prophase I during male meiosis: two adjacent but resolvable centriolar SPD-2 foci can be detected in nuclei in the transition zone (where nuclei are entering meiotic prophase) and in pachytene nuclei (in which homologs are fully paired and synapsed). Centriole-specific SPD-2 signals become transiently undetectable during the diplotene and karyosome stages and then reappear at diakinesis (the last stage of prophase I; Fig. 1*C*; Fig. S1). The SPD-2 IF signal then expands beyond the centriole foci starting in diakinesis and progressing through metaphase I; this recruitment of SPD-2 to the PCM is indicative of centrosome maturation (Fig. S1) (28). Pericentriolar SPD-2 IF signals shrink transiently during separation of the centriole pairs early in anaphase I, and then PCM-associated SPD-2 progressively expands until metaphase II (28) and persists through anaphase II. Pericentriolar SPD-2 then declines abruptly after anaphase II as the spermatids begin to bud off from the residual body (a modified cytokinesis that we will refer to as budding division), so that only the SPD-2 centriole foci are detected in the spermatids (Fig. 1*C*; Fig. S1). We note that in both mitosis and the first meiotic division, a decline in pericentriolar SPD-2 during anaphase is correlated with centriole disengagement (Fig. 1 *B* and *C*) (28, 29), whereas in the second meiotic division, pericentriolar SPD-2 persists during anaphase, and centrioles do not disengage (Fig. 1*C*) (31). Together, these observations confirm that centriole disengagement does not normally occur during the second meiotic division of *C. elegans* spermatocyte meiosis and raise the possibility that an active mechanism may be involved in maintaining engagement.

HORMA Proteins Prevent Centriole Separation During Meiosis II. Our analysis of spermatogenesis in *horma* mutants revealed an unanticipated role for the conserved meiosis-specific HORMA proteins HIM-3 and HTP-1/2 in preventing untimely separation of centrioles during the spermatocyte divisions (Fig. 2). Our high-resolution IF images of the SAS-4 centriolar protein revealed that *him-3* and *htp-1 htp-2* mutant spermatocytes at stages other than anaphase I frequently had two SAS-4 foci within a centrosome (Fig. 2*A*). Quantitation of this phenotype indicated that both the *him-3* and *htp-1 htp-2* null mutants exhibited significant increases in the proportions of meiosis II spindles in which one or both centrosomes contained two SAS-4 foci (Fig. 2*B*).

Centriole duplication and centrosome function appear to be normal in meiosis I in the *him-3* and *htp-1 htp-2* mutants (Fig. 2 *C*

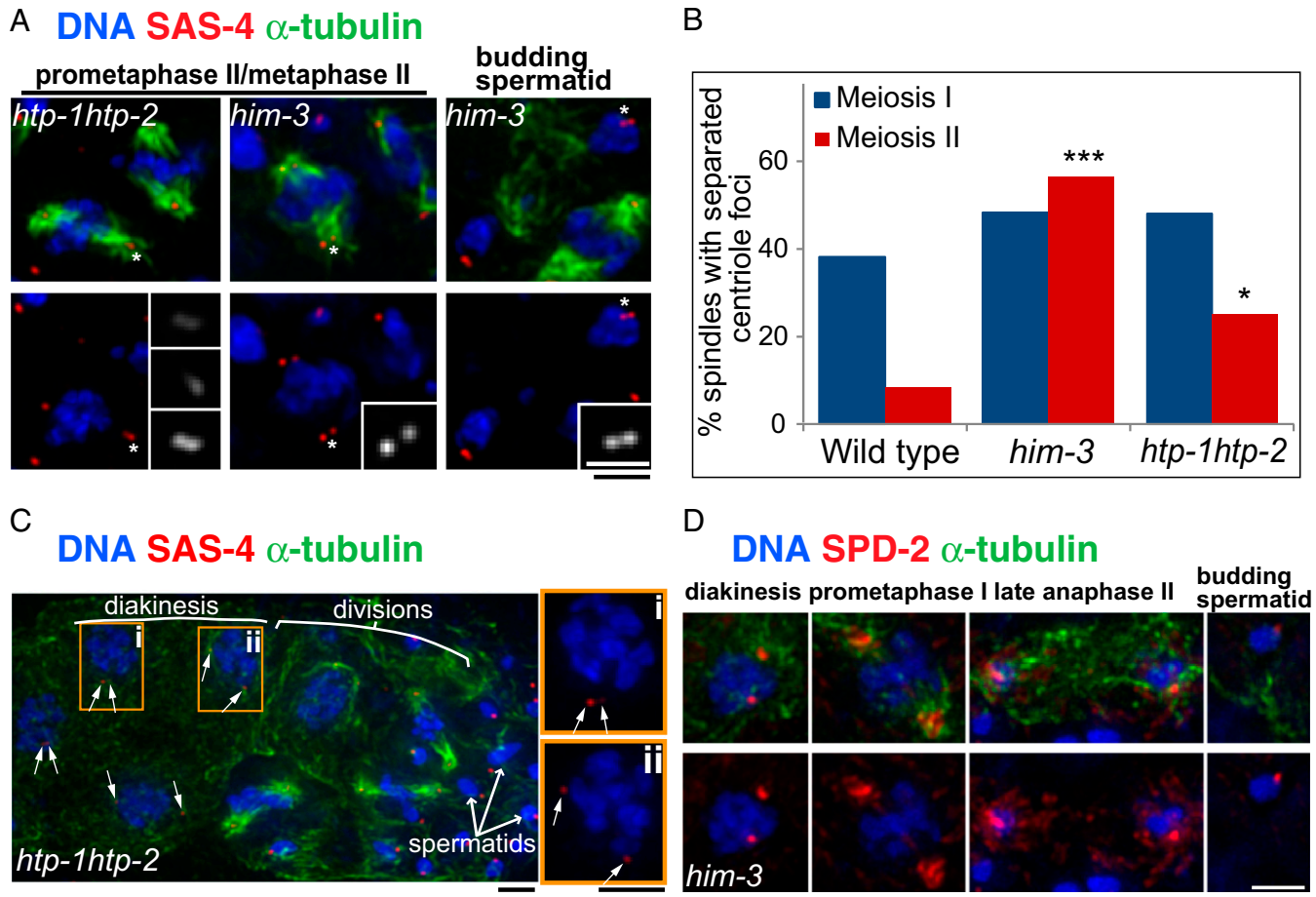

Fig. 2. Inappropriate separation of centrioles during the second meiotic divisions in *horma* mutant spermatocytes. (*A*, *C*, and *D*) Projections of immunofluorescence images of *htp-1 htp-2* and *him-3* mutant spermatocytes stained with α-tubulin, Hoechst, and α-SAS-4 (which localizes specifically to centrioles; *A* and *C*) or α-SPD-2 (which localizes both to centrioles and to pericentriolar material during some stages of the cell cycle; *D*). (*A*) Images show spermatocytes undergoing the second meiotic division. (*Left* and *Center*) Meiosis II spindles with a prometaphase/metaphase organization. (*Right*) Spermatids budding off from the residual body (modified cytokinesis). The images of SAS-4 in the *Insets* highlight the separated centriole foci at the spindle poles marked with asterisks; for the *htp-1 htp-2* image, *Insets* showing both the full projection (*Bottom*) and two different individual 0.1-μm-thick optical sections (*Top* and *Middle*) are provided. (Black scale bar, 2 μm; white scale bar for Inset images, 1 μm.) (*B*) Quantitation of the incidence of meiosis I and meiosis II spindles with separated centriole foci in WT, *him-3,* and *htp-1 htp-2* spermatocytes. ***$P = 0.0003$ and *$P < 0.02$ by Fisher exact test comparing mutants to WT. (*C*) Projection of a portion of an *htp-1 htp-2* mutant male gonad showing that spermatocyte nuclei enter the meiotic divisions with the normal number (two) of centriole foci (arrows). An early diakinesis nucleus and a late diakinesis nucleus are highlighted in *i* and *ii*, respectively. (Scale bars, 2 μm.) (*D*) SPD-2 immunofluorescence in *him-3 or htp-1 htp-2* mutant spermatocytes. Dynamic localization of SPD-2 parallels that in WT. Stages depicted are as follows: mid-diakinesis, in which SPD-2 localizes at the centrioles; prometaphase I, with SPD-2 present in the PCM, anaphase II, in which pericentriolar SPD-2 is still present (but is starting to decline); end of the budding division, in which only centriolar SPD-2 is detected. (Scale bar, 2 μm.)

and *D*), supporting the conclusion that the centrosome defects in these mutants originate after the first meiotic division. As in WT male meiosis, two discernible SAS-4 foci first become apparent early in prophase I, and these foci separate further and begin to nucleate microtubules by diakinesis (the end of prophase I; Figs. 1*B* and 2*C*). Further, the timing of centrosome maturation in meiosis I, as assessed by SPD-2 localization to the PCM, is also equivalent to that of WT (Figs. 2*D* and 1*C*). Moreover, our imaging included examples where we could unambiguously identify either (*i*) pairs of late anaphase II spindles that had arisen from the same meiocyte or (*ii*) four spermatids budding from the same residual body (Fig. S2). These examples provided definitive evidence that inappropriate separation of centriole foci could be detected in germ cells that were undergoing or had completed the meiosis II division. Given that the number and appearance of centrioles and centrosomes is normal before and during the meiosis I division, we conclude that the centrosome defects in *him-3* and *htp-1 htp-2* mutant spermatocytes arise during meiosis II.

We infer that the separated centriole foci in meiosis II represent abnormally disengaged centrioles based on multiple observations. First, separated SAS-4 foci within the centrosomes of the mutant secondary spermatocytes shown in Fig. 2*A* and those quantified in Fig. 2*B* are >260 nm apart (mean distance = 415 nm, $n = 26$). Because the *C. elegans* sperm centrioles are 150 nm long (7) and are arranged in a tight orthogonal configuration (6), pairs of SAS-4 foci with peak intensities that are separated by distances greater that 215 nm most likely represent pairs of centrioles that had become separated. Second, we never see either meiosis II spindles with more than two SAS-4 centriole foci per centrosome or budding spermatids with more than two centriole foci in the *horma* mutants. Moreover, in meiotic figures with pairs of late anaphase II spindles or with four spermatids budding from a single residual body, we readily detected more than four total SAS-4 foci, with either one or two SAS-4 foci associated with each spindle pole or budding spermatid (Fig. S2). This latter observation is inconsistent with pairs of SAS-4 foci having arisen either from centrosome missegregation or from

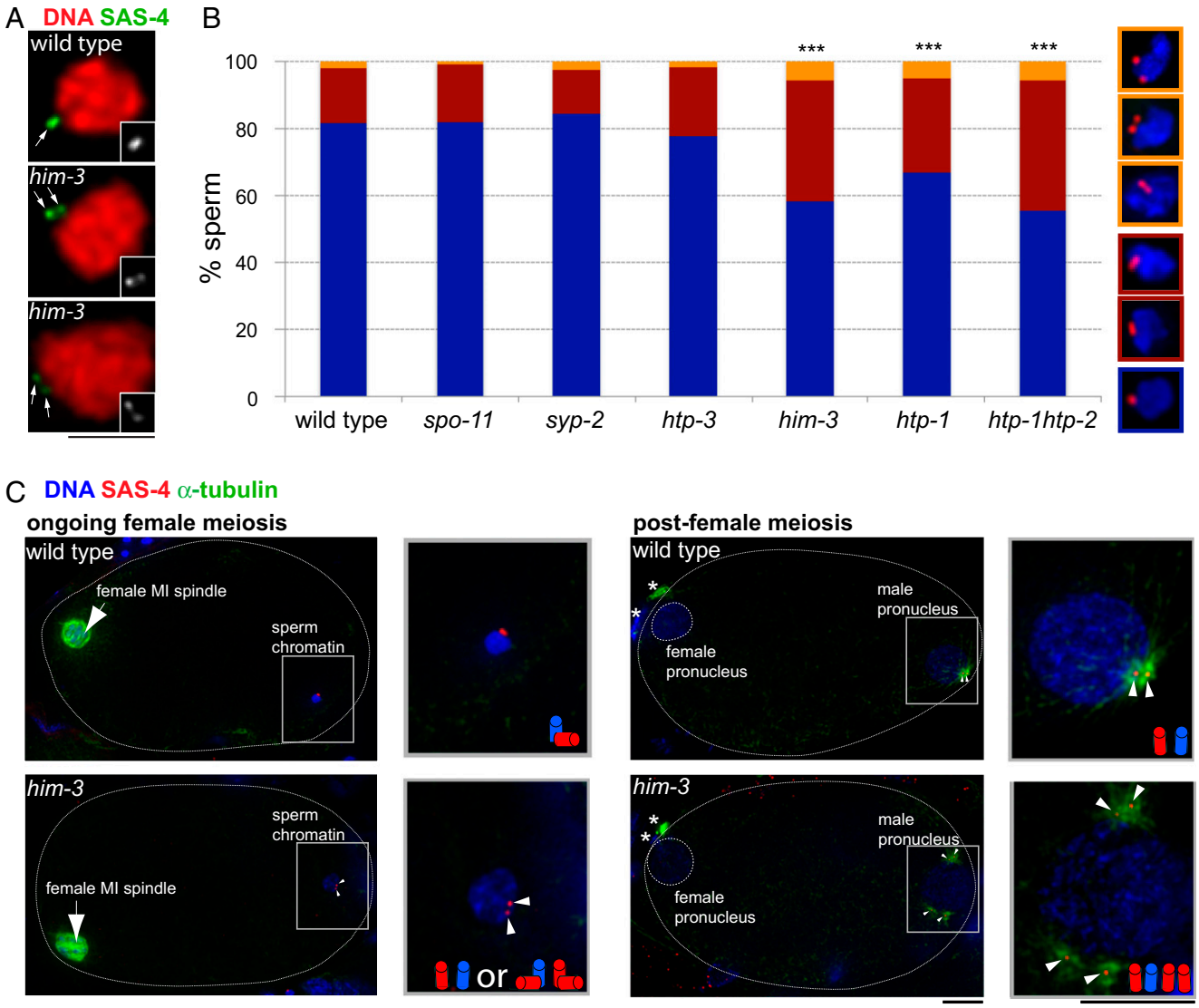

Fig. 3. Abnormal separation of centrioles during the *horma* mutant spermatocyte divisions results in sperm with separated centrioles and one-cell embryos with extra centrosomes. (*A*) Projections of STED superresolution immunofluorescence images of WT and mutant sperm stained with α-SAS-4 and DNA dye DRAQ5. Arrows mark centriole foci in *him-3* mutant sperm that are separated from each other by >220 nm. (Scale bar, 1 μm.) (*B*) Quantitation of centriole separation from standard high-resolution IF images, depicting the percent of WT or mutant sperm with two well-separated SAS-4 foci (class III), an elongated SAS-4 focus (class II, most of which represent separated centrioles), or a single round SAS-4 focus (class I); high-resolution IF images at the right of the graph show examples of each category. ***$P < 0.0001$ by χ^2 test comparing mutants to WT. (*C*) Projections of WT one-cell stage embryos (*Upper*) and *him-3* one-cell stage embryos derived from self-fertilized m+z- *him-3* hermaphrodites (*Lower*), with enlargements of the indicated regions. Embryos at the left are at an earlier stage, as indicated by the presence of female meiosis I spindles in the anterior of the newly fertilized embryos; arrowheads indicate the two well-separated centriole foci that are visible adjacent to the sperm chromatin mass in the *him-3* early embryo. The later embryos at the right have completed female meiosis and formed a female pronucleus. Whereas two centrosomes (each containing a single centriole focus) and microtubule asters are associated with the WT male pronucleus, four centrosomes (each containing a single centriole focus) and microtubule asters are associated with the *him-3* male pronucleus shown here. Enlargements include diagrams depicting the inferred organization of centrioles within the SAS-4 centriole foci detected adjacent to the corresponding male pronucleus. Arrowheads indicate centriole foci; asterisks mark the polar bodies. (Scale bar, 5 μm.)

a skipped meiotic division. Thus, we conclude that the pairs of centriole foci observed at meiosis II spindle poles and in budding spermatids reflect centriole pairs that had become disengaged during meiosis II. However, these data do not address whether or not these inappropriately disengaged centrioles had also undergone a single extra round of duplication after disengagement.

Although a decline in pericentriolar SPD-2 during anaphase is normally correlated with centriole disengagement (during mitosis and meiosis I) and persistence of pericentriolar SPD-2 during anaphase is correlated with a lack of disengagement during WT meiosis II, we found that pericentriolar SPD-2 also persisted during anaphase II in the *him-3* and *htp-1 htp-2* mutants (Fig. 2*D*). Thus, the inappropriate centriole disengagement that occurs during meiosis II in these mutants is not associated with a decline in pericentriolar SPD-2.

Separated Centriole Pairs in *him-3* and *htp-1 htp-2* Mutant Sperm. Consistent with centrioles having separated inappropriately during the second meiotic division, we frequently detected evidence of centriole separation in *him-3* and *htp-1 htp-2* mutant sperm. In stimulated emission depletion (STED) superresolution images of WT sperm ($n = 58$), a single SAS-4 focus was detected 79% of the time (Fig. 3*A*); further, in those WT sperm where two foci were evident (21%), such foci were usually only partially resolved (10/12).

In contrast, of the *horma* mutant sperm examined using STED imaging ($n = 96$), only 10% had a single SAS-4 focus, whereas the vast majority had either two well-resolved foci (59%; Fig. 3*A*) or two partially resolved foci (31%).

We used standard high-resolution imaging of SAS-4 IF to quantitate and compare the occurrence of centriole separation in WT sperm, *horma* mutant sperm, and sperm from several other classes of meiotic mutants (Fig. 3*B*). We scored three classes of SAS-4 centriole foci in these images: a single small round SAS-4 focus (class I), a long SAS-4 focus that was about the length of two normal SAS-4 foci (class II), and a pair of SAS-4 foci that were clearly separated (class III). In addition to the class III foci (clearly indicative of separated centrioles), we infer that the majority of class II foci also represent separated centrioles. This inference is based both on measurement of distances between local fluorescence intensity peaks near opposite ends of the class II foci (*Materials and Methods*) and on the much higher proportion of clearly resolved SAS-4 foci in *horma* mutant sperm in our STED superresolution images (Fig. 3*A*), which reflects an ability to resolve spatially separated foci that would have been scored as class II by standard high-resolution imaging. Both *him-3* and *htp-1 htp-2* mutant sperm exhibited an elevation of class II and class III SAS-4 foci, consistent with the STED imaging and with our observations of an elevated incidence of separated centriole foci during the meiosis II division in these mutants.

Importantly, this quantitation revealed that the centriole separation phenotype is specific to *him-3 and htp-1 htp-2* mutants and is not simply an indirect consequence of failure to form chiasmata during meiotic prophase, because the incidence of class II and class III foci in sperm from the *spo-11* mutant (which is defective in initiation of crossover formation) (32) and the *syp-2* mutant (which is defective in homologous chromosome synapsis and crossover formation) (33) did not differ significantly from WT sperm. In addition, we did not observe an increase in the incidence of class II or class III SAS-4 foci in mutants lacking HTP-3, another member of the meiotic HORMA domain protein family (18). Together our data indicate that the inappropriate separation of centrioles in *him-3* and *htp-1 htp-2* mutant spermatocytes reflects a specific role for the HIM-3 and HTP-1/2 proteins in maintaining engagement of the centrioles during the second meiotic division. Further, because HTP-3 is required for HIM-3 and HTP-1/2 localization onto chromosomes (18, 19), the lack of a centriole separation phenotype in the *htp-3* mutant implies that association of HIM-3 and HTP-1/2 with chromosomes is not essential for the function of these proteins in maintaining centriole engagement.

Premature Centriole Separation Results in a Subset of Zygotes with an Extra Pair of Centrosomes. We were able to infer the likely state of the centrioles (i.e., duplicated vs. not duplicated) that were provided by the sperm by examining their subsequent behavior in the zygotes. At fertilization, the WT sperm provides the oocyte with a single engaged centriole pair (7, 10, 11). This centriole pair remains engaged and associated with the sperm nucleus until female meiosis is nearly completed (Fig. 3*C*, *Upper Left*) (7). Once female meiosis achieves anaphase II, the centrioles disengage, but do not start to grow daughter centrioles until after the female meiotic divisions are completed and the female pronucleus becomes apparent (Fig. 3*C*, *Upper Right*). In contrast with the WT, where we usually observed only a single SAS-4 focus (associated with the sperm chromatin mass) in zygotes at stages before anaphase II of female meiosis (11/12), we frequently observed two separate SAS-4 foci associated with the sperm chromatin mass in *htp-1 htp-2* and *him-3* zygotes that were at earlier stages of female meiosis (Fig. 3*C*, *Lower Left*). Among the early (preanaphase II) *htp-1 htp-2* and *him-3* mutant zygotes scored, 7 of 14 had two separate SAS-4 foci, consistent with the frequency of separated centriole foci in sperm. Further, we never observed more than two SAS-4 foci in these early zygotes, and there was no evidence of premature recruitment of microtubules or PCM at this stage (indicating that precocious centrosome activation did not occur). These data imply that the centrioles were inherited from the sperm in an inactive state but do not distinguish whether the separated SAS-4 foci in these early zygote represented (*i*) a single prematurely disengaged centriole pair or (*ii*) two engaged centriole pairs brought in by a mutant sperm that had undergone a single extra centriole duplication event during the second spermatocyte division. However, based on examination of later zygotes (i.e., those that had completed meiosis and formed female pronuclei, but had not yet undergone pronuclear migration), we were able to infer that both classes of sperm were present. Sperm with single pair of prematurely disengaged centrioles that had not yet duplicated would yield the normal number of centrosomes (two) in late zygotes. However, sperm contributing two engaged centriole pairs would give rise to four centrosomes in late zygotes, as each pair of centrioles would disengage and then duplicate. As expected, we never detected more than two centrosomes in WT late zygotes ($n = 30$; Fig. 3*C*, *Upper Right*). In contrast, a subset of the *htp-1 htp-2* (2/8) and *him-3* (2/7) mutant late zygotes contained four centrosomes, indicating that some zygotes had resulted from fertilization by sperm carrying two engaged centriole pairs (Fig. 3*C*, *Lower Right*). Based on all of the above, we infer that the extra round of centriole duplication giving rise to such sperm and zygotes most likely occurred in spermatocytes during the second meiotic division. We suggest that if centriole disengagement occurs early enough during the second meiotic division, the cellular environment is competent to support an additional centriole duplication event prior to the budding division.

Maintenance of Centriole Engagement in Spermatocyte Meiosis Is Promoted by REC-8 Cohesin and Antagonized by Separase. Recent studies in other systems have provided evidence that cohesins localize to the centrosome during mitosis, that cohesins function in maintaining centriole engagement, and that centriole disengagement during mitosis is dependent on removal of cohesin by the protease separase (34, 35). Moreover, our own previous work had demonstrated that HTP-1/2 functions to prevent premature separation of sister chromatids during meiosis I in *C. elegans* by protecting REC-8 cohesin from separase-dependent removal (20). Thus, we investigated whether HORMA proteins might prevent centriole disengagement via a similar mechanism.

First, we found that, in addition to its localization on chromosomes during meiosis I, we can also detect specific HTP-1/2 localization at the centrosomes from late prophase (diakinesis) through anaphase II (Fig. 4*A*). This finding indicates that HTP-1/2 is present at the centrosomes in WT meiosis during stages of meiosis II where we see inappropriately separated centriole foci in the *htp-1 htp-2* mutant, consistent with HTP-1/2 functioning at the centrosomes to prevent untimely disengagement of centrioles.

Second, we demonstrated that REC-8 plays a role in maintaining centriole engagement during the male meiotic divisions by showing that spermatocytes and sperm from a mutant lacking REC-8 function (19, 36) exhibit premature centriole separation at frequencies comparable to those observed for *htp-1 htp-2* mutant spermatocytes and sperm (Fig. S3; Fig. 4*B*). Further, we also detected separated centriole foci associated with the sperm nucleus in 8 of 17 in *rec-8* null mutant early zygotes, and we detected four centrosomes in 3 of 13 *rec-8* late zygotes. These data support our hypothesis that cohesin complexes containing REC-8 function in preventing untimely separation of spermatocyte centrioles during the second meiotic division.

Third, we investigated whether separase is involved in centriole disengagement during male meiosis. Immunostaining of endogenous separase protein SEP-1 in spermatocytes revealed a dynamic localization of this protein on chromosomes and centrosomes.

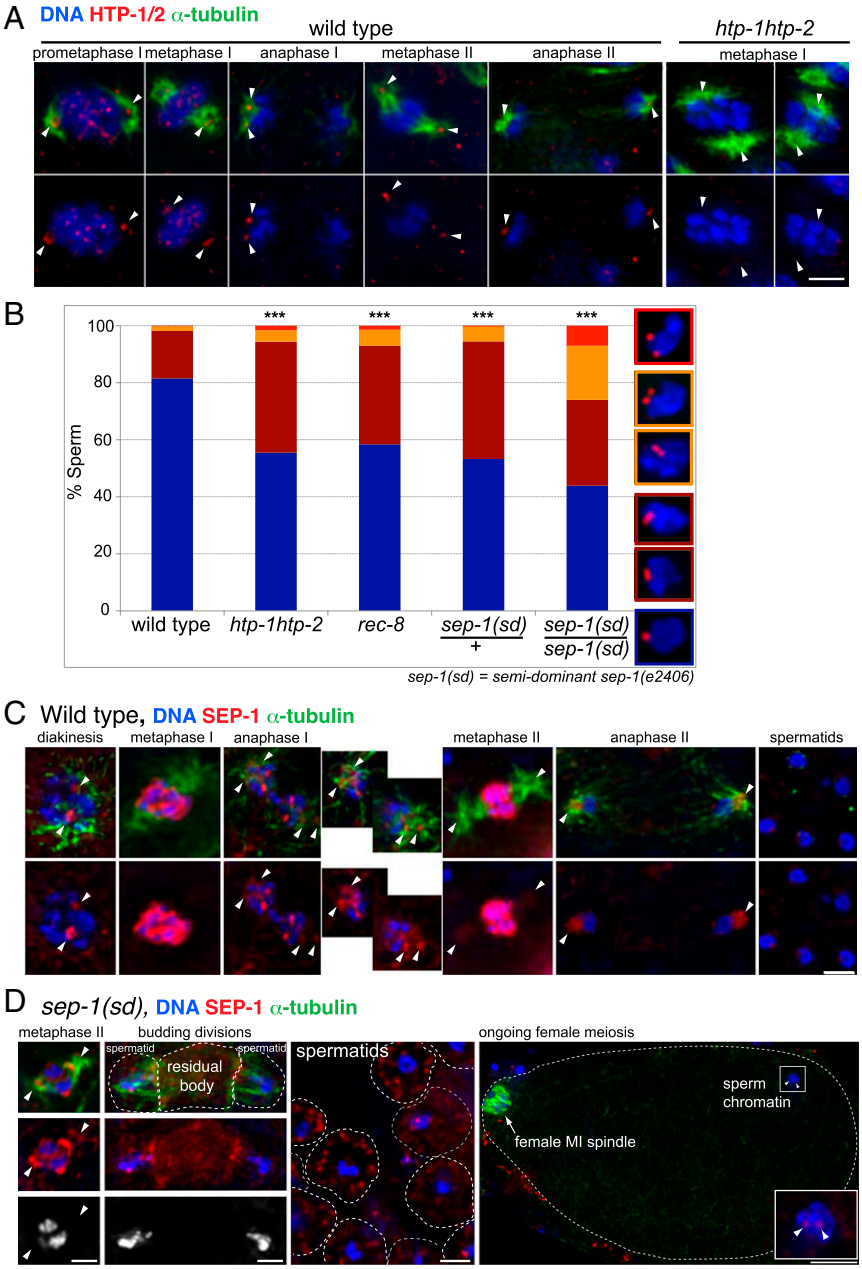

Fig. 4. Regulation of centriole engagement in spermatocyte meiosis. (*A*) Projections of IF images showing HTP-1/2 localized at the centrosomes throughout the spermatocyte meiotic division program in WT spermatocytes (and lack of immunostaining in *htp-1 htp-2* mutant spermatocytes). HTP-1/2 is present both on the chromosomes and at the centrosomes during prometaphase I and metaphase I and then is lost from the chromosomes at anaphase I but continues to be detected at centrosomes through anaphase II. (*B*) Quantitation of the percent of WT or mutant sperm exhibiting the indicated categories of SAS-4 foci. Categories are as in Fig. 3*B*, except that the class III category is further subdivided to highlight a subclass with widely separated foci. *sep-1(sd)* indicates use of the *sep-1(e2406)* allele, which exhibits a semidominant effect attributable to elevated local SEP-1 activity. ***$P < 0.0001$ by χ^2 tests comparing mutants to WT. (*C*) Projections of IF images showing localization of WT SEP-1 protein in dividing spermatocytes and spermatids. To the right of the anaphase I image, partial projections of each of its spindle poles are shown to emphasize the presence of SEP-1 at the centrosomes. (Note: the field of spermatids shown is derived from a composite image.) (*D*) Projections of IF images showing localization of the mutant SEP-1 protein in *sep-1(sd)* dividing spermatocytes, spermatids, and a one-cell embryo. In the *sep-1(sd)* metaphase II spindle shown, the mutant SEP-1 protein is detected not only around the chromosomes but also at the spindle poles. In the *sep-1(sd)* budding spermatocyte shown, the majority of the mutant SEP-1 protein is discarded into the residual body (as in WT meiosis); however, substantial SEP-1 is also detected in the budding spermatids and mature sperm. In the *sep-1(sd)* early one-cell stage embryo shown, two SEP-1 foci are detected adjacent to the sperm pronucleus (highlighted by arrowheads). In *A*, *C*, and *D*, arrowheads indicate centrosomes. (Scale bars, 2 μm.)

Endogenous SEP-1 is detected in the germ cell cytoplasm throughout most of meiotic prophase I (Fig. S4*A*). Spermatocytes in the diplotene stage of prophase I accumulate low levels of SEP-1 in puncta around the nuclear envelope (Fig. S4*A*). At diakinesis, the latest stage of prophase I before nuclear envelope breakdown, SEP-1 becomes enriched at the centrosomes (Fig. 4*C*). Upon nuclear envelope breakdown, SEP-1 at the centrosomes diminishes to nearly undetectable levels, and SEP-1 becomes highly enriched around each chromosome (metaphase I in Fig. 4*C*). At anaphase I, chromosomal SEP-1 is diminished and SEP-1 again

becomes highly enriched on the centrosomes. At metaphase II, SEP-1 becomes nearly undetectable at the centrosomes and enriched at the chromosomes (Fig. 4*C*). Departure of SEP-1 from the chromosomes occurs again at anaphase II, concomitant with transient enrichment of SEP-1 once more on the centrosomes. Finally, much of the SEP-1 protein is discarded into the residual body during the budding division, so that SEP-1 becomes nearly undetectable in spermatids that have completed the budding process (Fig. S4*B*; Fig. 4*C*). We observe similar dynamic localization by IF of GFP::SEP-1 expressed from a transgene that has been reported to rescue the *sep-1* loss of function phenotypes (Fig. S4*C*) (37). These data indicate that separase is present and potentially available to promote centriole disengagement during meiosis II (as it does during mitosis in other systems) (35, 38, 39), even though it normally does not do so in *C. elegans* secondary spermatocytes.

Analysis of spermatocytes carrying the *sep-1(e2406)* allele, a temperature-sensitive missense mutation affecting the SEP-1 protein (40), provided direct evidence that separase activity can indeed provoke inappropriate disengagement of centrioles during spermatocyte meiosis. *C. elegans* SEP-1 has been shown to have prominent roles both in chromosome segregation and in membrane trafficking associated with both cortical granule exocytosis and cytokinesis in embryos (37, 40). *sep-1(e2406)* is a separation-of-function mutant that is largely proficient for chromosome segregation but is profoundly defective for cortical granule exocytosis and cytokinesis (40, 41). Moreover, the defects in this mutant appear to reflect the ability of the mutant SEP-1 protein to localize to relevant structures within the cell: whereas SEP-1 colocalization with cortical granules is lost in *sep-1(e2406)* embryos, SEP-1 is still able to localize to the oocyte anaphase I spindle (37). In contrast to the loss of SEP-1 localization at embryonic cortical granules, we found that SEP-1 exhibits an elevated local concentration at centrosomes in *sep-1(e2406)* mutant spermatocytes: whereas WT SEP-1 localized to spermatocyte centrosomes only during late prophase and anaphase, the mutant SEP-1 protein was present at detectable levels on the centrosomes throughout the spermatocyte divisions (Fig. 4*D*). Further, although much of the mutant SEP-1 protein is discarded into the residual body, SEP-1 protein persists at higher levels in mutant sperm than in WT sperm, and we detect two SEP-1 foci near the sperm chromatin mass in newly fertilized *sep-1(e2406)* mutant embryos (Fig. 4*D*) but not in WT embryos of the same stage. These localization data raised the possibility that the *sep-1(e2406)* mutation acts as a centrosome-specific gain-of-function mutation, leading to locally elevated levels of SEP-1 activity at the centrosomes. Indeed, we found that sperm from *sep-1(e2406)* homozygous mutant worms exhibited a high frequency of sperm with class III and class II SAS-4 foci, indicating premature separation of centrioles (Fig. 4*B*). Further, the *sep-1(e2406)* mutation exhibited a semidominant effect, also eliciting significantly elevated levels of separated centrioles in sperm from *sep-1(e2406)*/+ heterozygotes (Fig. 4*B*). The simplest interpretation of these data are that the *sep-1(e2406)* mutation results in locally elevated and/or persistent SEP-1 activity at centrosomes and that this elevated/persistent separase activity is sufficient to overcome the HORMA- and REC-8–dependent mechanisms that would normally enable centrioles to remain engaged until after fertilization.

As expected based on the observation of separated centrioles in sperm, we also detected separated centriole foci associated with the sperm chromatin in early zygotes from *sep-1(e2406)*/+ heterozygous hermaphrodites. Although separated centriole foci were observed in eight of eight of early zygotes imaged, late zygotes with four centrosomes were not observed (0 of 14). We speculate that centriole disengagement elicited by the mutant SEP-1 protein occurs slightly later than in the *horma* and *rec-8* mutants, likely because the HORMA-dependent protection machinery is still present in *sep-1* mutant spermatocytes and may succeed in delaying centriole pair disengagement long enough to prevent the abnormal duplication event observed in *horma* and *rec-8* mutants.

Conclusions. Together, our data support a model in which the meiotic HORMA domain proteins HIM-3 and HTP-1/2 function to maintain centriole engagement during meiosis II in spermatocytes and in sperm, likely by potentiating the activity of REC-8 cohesin in mediating engagement. In principle, the HORMA proteins could function in this capacity by promoting association of REC-8 with centrioles and/or by antagonizing separase-mediated REC-8 removal. We cannot exclude the former possibility, as REC-8 localization throughout the meiotic spindles and centrosomes (Fig. S5) makes it difficult to assess the requirements for REC-8 localization at the centrioles per se. However, REC-8 localization on the chromosomes does not require either HIM-3 or HTP-1/2 (19). Further, additional considerations lead us to favor the interpretation that the HORMA proteins prevent inappropriate centriole disengagement by locally inhibiting separase-dependent removal of REC-8.

First, HTP-1/2 is localized at spermatocyte centrosomes during the meiosis II division, placing this protein in the right place at the time when inhibition of separase activity is required to maintain centriole engagement. Moreover, a scheme in which HTP-1/2 prevents centriole separation during meiosis II by inhibiting REC-8 removal would precisely parallel the previously demonstrated role for HTP-1/2 in preventing premature separation of sister chromatids during meiosis I (20). Further, our evidence for repeated use of this HORMA-dependent strategy during *C. elegans* spermatocyte meiosis complements and extends recent studies in human cell culture showing that the maintenance and release of connections between sister chromatids and between centrioles are mechanistically linked (5, 35, 38).

Our data emphasize the fact that entire biological subroutines can be recruited to accomplish distinct tasks that require similar regulatory logic. In this case, the task is to temporarily maintain connections between structures that are ultimately destined for regulated separation. For mitotic cells, it had been suggested that the use of cohesin and separase to regulate both sister chromatid cohesion and centriole engagement might function as a means to couple the two types of separation events temporally during the cell cycle (35). However, HORMA-dependent mechanisms operate to maintain connections between sister chromatids during meiosis I and to maintain connections between centrioles during meiosis II, in both cases preventing inappropriate separation events that could potentially impair the subsequent cell division. Therefore, in the context of the HORMA-dependent cohesin maintenance strategy that we discovered, it is clear that parallel regulatory logic, rather than temporal coordination, is the relevant underlying commonality that drove its dual use in regulating both chromosome and centriole separation.

Materials and Methods

Strains, Culture Methods, and Genetics. *C. elegans* strains were cultured at 20 °C under standard conditions (42) unless otherwise noted. In addition to the WT strain Bristol N2, the following mutations and chromosome rearrangements were used: *LG I: sep-1(e2406), htp-3(y428), hT2[bli-4(e937) let-?(q782) qIs48)](I;III); LG III: unc-119(ed3); LG IV: htp-1(gk174), htp-2(tm2543), him-3(gk149), spo-11(ok79), rec-8(ok978), nT1[unc-?(n754) let-?(m435)](IV;V), nT1[unc-?(n754) let-? qIs50](IV;V); LG V: syp-2(ok307).* Meiotic mutations in the above strains are canonical nulls, except for *sep-1(e2406),* which is a temperature-sensitive allele that affects protein localization. For analysis of centriole foci in sperm from worms carrying the *sep-1(e2406)* mutation, worms were maintained at 15 °C and then shifted to 25 °C for 5–6 h before dissection. For analysis of centrioles in zygotes produced by *sep-1(e2406)*/+ hermaphrodites, worms were raised at 15 °C until the L3 larval stage and then shifted to 25 °C or 20 °C for about 24 h prior to dissection at the adult stage. A strain expressing the GFP::SEP-1 extrachromosomal array *ojEx64*

[pie-1P::gfp::sep-1; unc-119(+)] was shifted from 20 °C to 25 °C for 4 h before dissection to increase fluorescence intensity.

Cytological Analyses. Immunostaining of dissected gonads from N2 males, hermaphrodites, and embryos was as previously described (43, 44) with minor modifications. Gonads from L4 hermaphrodites or young adult males were dissected, fixed, and permeabilized by freeze-cracking in liquid nitrogen followed by soaking in methanol at −20° C (43) for 30 min. Embryos and gonads were rehydrated in PBS, blocked in AbDil [PBS plus 2% (wt/vol) BSA, 0.1% Triton X-100] as described by Oegema et al. (44), and incubated at 4° overnight with a combination of different primary antibodies. The following primary antibodies were used at the indicated dilutions: α-HTP-1/2 (1:200) (20), α-REC-8 (1:100; CIM, Arizona State University), α-SEP-1 (1:250) (41), α-SAS-4 (1:1,000) (45), α-SPD-2 (1:1,000) (28), and anti–α -tubulin (1:1,000; FITC-conjugated DM1A from Sigma). After washing with PBST (PBS plus 0.1% Triton X-100), gonads were incubated with PBST containing 1 mg/mL Hoechst 33258 (Sigma) and mounted in 0.5% *p*-phenylenediamine, 20 mM Tris-HCl, pH 8.8, and 90% (wt/vol) glycerol (44). Images were obtained as stacks of optical sections acquired at 0.1-μm intervals using the Deltavision deconvolution microscopy system. For STED superresolution microscopy, the following modifications were used: α-SAS-4 was used at 1:1,500 dilution, and the DNA dye used was DRAQ5. Samples were mounted with Prolong containing antifade (Invitrogen). Optical sections were acquired at 0.2-μm intervals using the Leica Microsystems TCS STED CW superresolution microscope system. Deconvolution of STED images was performed using Volocity software (PerkinElmer).

Quantitation of SAS-4 Centriole Foci. Primary and secondary spermatocytes were identified by their position in the gonad, by the structure of their chromosomes, and by spindle size and morphology; moreover, meiosis II spindles were also distinguished from meiosis I spindles by the presence (during meiosis II) of two adjacent synchronous meiotic figures, as depicted in Fig. 1*A*. This latter criterion was particularly useful in meiotic mutants in which the number of chromosomes present at meiosis II was variable because of chromosome mis-segregation during meiosis I. The proportions of dividing spermatocytes in meiosis I and meiosis II in *horma* mutants were similar to WT, suggesting that the relative timing of the meiotic divisions in the *horma* mutant spermatocytes is normal (Table S1). Separation of fluorescent SAS-4 centriole foci at spindle poles was assessed by scanning through stacks of optical sections encompassing the spindles. Foci were scored as separated when they could be distinguished as two individual fluorescence spots when scanning through consecutive optical sections. Distances between peak fluorescence intensities of separated foci were measured using SoftWoRx Suite software.

SAS-4 foci in sperm were scored by scanning through consecutive optical sections and were classified into categories as described above. We also measured distances between local fluorescence intensity peaks near opposite ends of the class II foci to provide additional support for the conclusion that most class II foci represent disengaged centriole pairs. Average interpeak distances (±SD) for class II foci were as follows: 370 ± 140 nm (n = 30) for WT sperm; 430 ± 110 nm (n = 79) for *him-3* mutant sperm; and 370 ± 70 nm (n = 79) for *htp-1 htp-2* mutant sperm. Further, interpeak distances were never less than 220 nm apart in the *horma* mutant sperm, indicating that most or all class II foci detected in these mutants represent disengaged centrioles. The majority of class II foci in WT sperm also had interpeak distances >220 nm, implying that a subset of WT sperm may also have disengaged centrioles; however, 17% of the WT sperm scored as class II had interpeak distances <200 nm, likely reflecting centriole pairs that were still engaged. We also measured distances between peak intensities of the two separated SAS-4 foci in class III sperm; average interpeak distances were 570 ± 170 nm (n = 17) for *him-3* and 470 ± 200 nm for *htp-1 htp-2* (n = 19).

Staging of One-Cell Embryos. The status of centrioles/centrosomes was evaluated in zygotes at two stages: (*i*) prior to anaphase II (early) and (*ii*) after the female pronucleus had formed but before it had migrated >1.5 nuclear diameters from the anterior cortex. Further, within this second category, the WT and *him-3* embryos shown in the right half of Fig. 3*C* were determined to be closely stage-matched based on several criteria (as depicted in Fig. S6): (*i*) measured distance between the female pronucleus and the anterior cortex of the embryo (indicating the extent of pronucleus migration); (*ii*) measured distance between the separating pairs of centrosomes associated with the male pronucleus (one pair in the WT, two pairs in the *him-3* mutant), reflecting the extent of centrosome migration; and (*iii*) the appearance of the microtubule asters associated with the centrosomes (which become denser as more microtubules are recruited).

ACKNOWLEDGMENTS. We thank K. Oegema, A. Golden, and K. O'Connell for antibodies; K. Hillers, T. Stearns, and B. Roelens for comments on the manuscript; members of the A.M.V. laboratory for helpful discussions; D. Castaneda-Castellanos of Leica Microsystems for access to and assistance with the STED microscope; and the Caenorhabditis Genetics Center for strains. This work was supported by National Institutes of Health Grant R01 GM53804 (to A.M.V.) and a Canadian Institute of Health Research postdoctoral fellowship (to M.S.).

1. Manandhar G, Schatten H, Sutovsky P (2005) Centrosome reduction during gametogenesis and its significance. *Biol Reprod* 72(1):2–13.
2. Nigg EA, Stearns T (2011) The centrosome cycle: Centriole biogenesis, duplication and inherent asymmetries. *Nat Cell Biol* 13(10):1154–1160.
3. Wong C, Stearns T (2003) Centrosome number is controlled by a centrosome-intrinsic block to reduplication. *Nat Cell Biol* 5(6):539–544.
4. Tsou M-FB, et al. (2009) Polo kinase and separase regulate the mitotic licensing of centriole duplication in human cells. *Dev Cell* 17(3):344–354.
5. Tsou M-FB, Stearns T (2006) Mechanism limiting centrosome duplication to once per cell cycle. *Nature* 442(7105):947–951.
6. Albertson DG, Thomson JN (1993) Segregation of holocentric chromosomes at meiosis in the nematode, Caenorhabditis elegans. *Chromosome Res* 1(1):15–26.
7. Pelletier L, O'Toole E, Schwager A, Hyman AA, Müller-Reichert T (2006) Centriole assembly in Caenorhabditis elegans. *Nature* 444(7119):619–623.
8. Leidel S, Gönczy P (2003) SAS-4 is essential for centrosome duplication in C elegans and is recruited to daughter centrioles once per cell cycle. *Dev Cell* 4(3):431–439.
9. O'Connell KF, et al. (2001) The C. elegans zyg-1 gene encodes a regulator of centrosome duplication with distinct maternal and paternal roles in the embryo. *Cell* 105(4):547–558.
10. Wolf N, Hirsh D, McIntosh JR (1978) Spermatogenesis in males of the free-living nematode, Caenorhabditis elegans. *J Ultrastruct Res* 63(2):155–169.
11. Albertson DG (1984) Formation of the first cleavage spindle in nematode embryos. *Dev Biol* 101(1):61–72.
12. Schvarzstein M, Wignall SM, Villeneuve AM (2010) Coordinating cohesion, co-orientation, and congression during meiosis: Lessons from holocentric chromosomes. *Genes Dev* 24(3): 219–228.
13. Couteau F, Zetka M (2005) HTP-1 coordinates synaptonemal complex assembly with homolog alignment during meiosis in C. elegans. *Genes Dev* 19(22):2744–2756.
14. Martinez-Perez E, Villeneuve AM (2005) HTP-1-dependent constraints coordinate homolog pairing and synapsis and promote chiasma formation during C. elegans meiosis. *Genes Dev* 19(22):2727–2743.
15. Zetka MC, Kawasaki I, Strome S, Müller F (1999) Synapsis and chiasma formation in Caenorhabditis elegans require HIM-3, a meiotic chromosome core component that functions in chromosome segregation. *Genes Dev* 13(17):2258–2270.
16. Couteau F, Goodyer W, Zetka M (2004) Finding and keeping your partner during meiosis. *Cell Cycle* 3(8):1014–1016.
17. Couteau F, Nabeshima K, Villeneuve A, Zetka M (2004) A component of C. elegans meiotic chromosome axes at the interface of homolog alignment, synapsis, nuclear reorganization, and recombination. *Curr Biol* 14(7):585–592.
18. Goodyer W, et al. (2008) HTP-3 links DSB formation with homolog pairing and crossing over during C. elegans meiosis. *Dev Cell* 14(2):263–274.
19. Severson AF, Ling L, van Zuylen V, Meyer BJ (2009) The axial element protein HTP-3 promotes cohesin loading and meiotic axis assembly in C. elegans to implement the meiotic program of chromosome segregation. *Genes Dev* 23(15):1763–1778.
20. Martinez-Perez E, et al. (2008) Crossovers trigger a remodeling of meiotic chromosome axis composition that is linked to two-step loss of sister chromatid cohesion. *Genes Dev* 22(20):2886–2901.
21. Kitajima TS, Kawashima SA, Watanabe Y (2004) The conserved kinetochore protein shugoshin protects centromeric cohesion during meiosis. *Nature* 427(6974):510–517.
22. Kitajima TS, Ohsugi M, Ellenberg J (2011) Complete kinetochore tracking reveals error-prone homologous chromosome biorientation in mammalian oocytes. *Cell* 146(4):568–581.
23. Kateneva AV, Higgins JMG (2009) Shugoshin and PP2A: Collaborating to keep chromosomes connected. *Dev Cell* 17(3):303–305.
24. Kerrebrock AW, Miyazaki WY, Birnby D, Orr-Weaver TL (1992) The Drosophila mei-S332 gene promotes sister-chromatid cohesion in meiosis following kinetochore differentiation. *Genetics* 130(4):827–841.
25. Ishiguro T, Tanaka K, Sakuno T, Watanabe Y (2010) Shugoshin-PP2A counteracts casein-kinase-1-dependent cleavage of Rec8 by separase. *Nat Cell Biol* 12(5):500–506.
26. de Carvalho CE, et al. (2008) LAB-1 antagonizes the Aurora B kinase in C. elegans. *Genes Dev* 22(20):2869–2885.
27. Kirkham M, Müller-Reichert T, Oegema K, Grill S, Hyman AA (2003) SAS-4 is a C. elegans centriolar protein that controls centrosome size. *Cell* 112(4):575–587.
28. Kemp CA, Kopish KR, Zipperlen P, Ahringer J, O'Connell KF (2004) Centrosome maturation and duplication in C. elegans require the coiled-coil protein SPD-2. *Dev Cell* 6(4):511–523.
29. Pelletier L, et al. (2004) The Caenorhabditis elegans centrosomal protein SPD-2 is required for both pericentriolar material recruitment and centriole duplication. *Curr Biol* 14(10):863–873.

30. Zhu F, et al. (2008) The mammalian SPD-2 ortholog Cep192 regulates centrosome biogenesis. *Curr Biol* 18(2):136–141.
31. Shakes DC, et al. (2009) Spermatogenesis-specific features of the meiotic program in Caenorhabditis elegans. *PLoS Genet* 5(8):e1000611.
32. Dernburg AF, et al. (1998) Meiotic recombination in C. elegans initiates by a conserved mechanism and is dispensable for homologous chromosome synapsis. *Cell* 94(3):387–398.
33. Colaiácovo MP, et al. (2003) Synaptonemal complex assembly in C. elegans is dispensable for loading strand-exchange proteins but critical for proper completion of recombination. *Dev Cell* 5(3):463–474.
34. Guan J, Ekwurtzel E, Kvist U, Yuan L (2008) Cohesin protein SMC1 is a centrosomal protein. *Biochem Biophys Res Commun* 372(4):761–764.
35. Schöckel L, Möckel M, Mayer B, Boos D, Stemmann O (2011) Cleavage of cohesin rings coordinates the separation of centrioles and chromatids. *Nat Cell Biol* 13(8):966–972.
36. Hayashi M, Chin GM, Villeneuve AM (2007) C. elegans germ cells switch between distinct modes of double-strand break repair during meiotic prophase progression. *PLoS Genet* 3(11):e191.
37. Bembenek JN, White JG, Zheng Y (2010) A role for separase in the regulation of RAB-11-positive vesicles at the cleavage furrow and midbody. *Curr Biol* 20(3):259–264.
38. Nakamura A, Arai H, Fujita N (2009) Centrosomal Aki1 and cohesin function in separase-regulated centriole disengagement. *J Cell Biol* 187(5):607–614.
39. Tsou M-FB, Stearns T (2006) Controlling centrosome number: Licenses and blocks. *Curr Opin Cell Biol* 18(1):74–78.
40. Siomos MF, et al. (2001) Separase is required for chromosome segregation during meiosis I in Caenorhabditis elegans. *Curr Biol* 11(23):1825–1835.
41. Bembenek JN, et al. (2007) Cortical granule exocytosis in C. elegans is regulated by cell cycle components including separase. *Development* 134(21):3837–3848.
42. Brenner S (1974) The genetics of Caenorhabditis elegans. *Genetics* 77(1):71–94.
43. Gönczy P, et al. (1999) Dissection of cell division processes in the one cell stage Caenorhabditis elegans embryo by mutational analysis. *J Cell Biol* 144(5): 927–946.
44. Oegema K, Desai A, Rybina S, Kirkham M, Hyman AA (2001) Functional analysis of kinetochore assembly in Caenorhabditis elegans. *J Cell Biol* 153(6):1209–1226.
45. Delattre M, et al. (2004) Centriolar SAS-5 is required for centrosome duplication in C. elegans. *Nat Cell Biol* 6(7):656–664.